# Tsunamis and splay fault dynamics

James Wendt,[1] David D. Oglesby,[2] and Eric L. Geist[3]

Received 23 March 2009; revised 10 June 2009; accepted 15 June 2009; published 4 August 2009.

[1] The geometry of a fault system can have significant effects on tsunami generation, but most tsunami models to date have not investigated the dynamic processes that determine which path rupture will take in a complex fault system. To gain insight into this problem, we use the 3D finite element method to model the dynamics of a plate boundary/splay fault system. We use the resulting ground deformation as a time-dependent boundary condition for a 2D shallow-water hydrodynamic tsunami calculation. We find that if the stress distribution is homogeneous, rupture remains on the plate boundary thrust. When a barrier is introduced along the strike of the plate boundary thrust, rupture propagates to the splay faults, and produces a significantly larger tsunami than in the homogeneous case. The results have implications for the dynamics of megathrust earthquakes, and also suggest that dynamic earthquake modeling may be a useful tool in tsunami research. **Citation:** Wendt, J., D. D. Oglesby, and E. L. Geist (2009), Tsunamis and splay fault dynamics, *Geophys. Res. Lett.*, *36*, L15303, doi:10.1029/2009GL038295.

## 1. Introduction

[2] Numerical models are a key means by which tsunami runup forecasts are determined. Typically, such tsunami models use detailed data on seafloor and shoreline topography to estimate the damage from potential future tsunamis [e.g., *Imamura and Shuto*, 1993; *Satake*, 1995; *Bourgeois et al.*, 1999]. Since earthquakes are among the most common sources of tsunamis, elastic models of seafloor displacement dictate the initial conditions for most tsunami hydrodynamic models. It is generally understood that the temporal details of the earthquake rupture and slip process are not very significant in tsunami generation and propagation, especially in the far field, because typical tsunami periods are significantly longer than the rupture and slip time scales of earthquakes. For this reason, and for general simplicity, most earthquake-related tsunami generation models use kinematic dislocation models for fault slip to produce a final static seafloor deformation pattern. Such a methodology assumes that one knows the earthquake size and slip pattern *a priori*. Unfortunately, in many locations there is very little information to guide one's choice of earthquake size and slip distribution. Dynamic spontaneous earthquake rupture models [e.g., *Andrews*, 1976b; *Das*, 1981; *Day*, 1982] can help alleviate this uncertainty: by using known fault geometry, material properties, and an assumed stress field, dynamic earthquake models will produce as their output the spatio-temporal evolution of earthquake rupture and slip, including the rupture path and the final earthquake size in geometrically complex fault systems. Of course, the inputs to dynamic rupture models have their own considerable uncertainties, but they help delineate possible faulting behaviors in a physically consistent manner and guide seafloor displacement estimation. As we will see below, different assumptions about fault stress patterns can lead to very different dynamic faulting behavior, and thus can have significant effects on tsunami generation and propagation, especially in the near field.

[3] The present work is among the first to use dynamic earthquake rupture models for tsunami simulation in subduction zones in the presence of splay faults. The presence of splay faults has been interpreted from a number of geophysical studies and has been suggested to strongly increase tsunami height [e.g., *Fukao*, 1979; *Geist and Yoshioka*, 1996; *Cummins and Kaneda*, 2000; *Park et al.*, 2002; *Baba et al.*, 2006; *Mukoyoshi et al.*, 2006; *Moore et al.*, 2007]. We take as a test case a geometry motivated by the 1946 Nankai Earthquake, which may have ruptured both the plate boundary thrust and a system of splay faults that cut the accretionary wedge [*Cummins and Kaneda*, 2000]. Using dynamic earthquake models and tsunami models, we answer two questions: 1) Under what conditions will an earthquake propagate to a splay fault instead of (or in addition to) the main plate boundary thrust? 2) What is the resultant effect on tsunami generation and propagation toward a nearby shore? We aim to show that dynamic models add an important new dimension to tsunami studies, and complement existing tsunami modeling methods.

## 2. Methods

[4] We use the 3D explicit finite element method [*Whirley and Engelmann*, 1993; *Oglesby*, 1999] to model the dynamics of the splay fault geometry illustrated in Figure 1. This model is motivated by the splay fault geometry inferred by *Cummins and Kaneda* [2000] for the 1946 Nankai earthquake, but for computational reasons it is significantly smaller along strike; it should be understood that our model is generic and not meant to reproduce this specific earthquake. The fault system consists of a shallow-dipping plate boundary thrust, with a two-segment, more steeply-dipping splay fault. Our faulting model assumes a slip-weakening friction law [*Ida*, 1972; *Palmer and Rice*, 1973; *Andrews*, 1976a] in which the frictional strength is directly proportional to the (time-dependent) normal stress. For simplicity we assume a linearly elastic homogeneous half-space for our faulting model, with physical and computational parameters shown in Table 1. After artificially nucleating rupture at the hypocenter (61 km down-dip, 32 km along strike on the plate boundary thrust, as shown in Figure 2), the

[1]Department of Physics, Pomona College, Claremont, California, USA.
[2]Department of Earth Sciences, University of California, Riverside, California, USA.
[3]U.S. Geological Survey, Menlo Park, California, USA.


0094-8276/09/2009GL038295

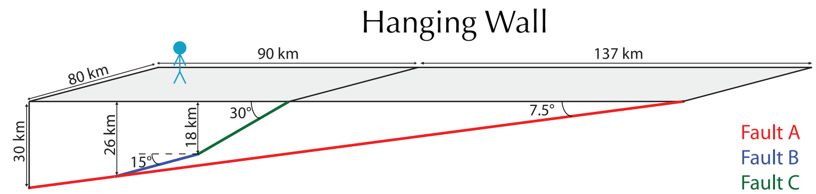


**Figure 1.** Cartoon of fault geometry.

subsequent evolution of rupture and slip is calculated by the finite element method with no further intervention. A key ingredient in any dynamic faulting model is the stress field on the fault system. A typical approach is to use a regional (triaxial) stress field that is resolved onto the fault segments, with different shear and normal stresses on each segment according to its orientation [e.g., *Aochi et al.*, 2002; *Kame et al.*, 2003; *Oglesby*, 2005]. However, in a splay fault system such as in the current model, such an assumption is difficult to implement: because of its low dip angle, the plate boundary thrust is nearly parallel to one of the principle compressive stresses. Most models with a constant regional stress field and homogeneous frictional properties that allow this fault to rupture will produce instantaneous slip over the more favorably-oriented splay faults. Thus, we make the somewhat arbitrary choice for a stress field on our 3 fault segments that is motivated by a regional stress field, but with increasing normal stress with depth on the splay faults and reduced normal stress on the plate boundary thrust. A potential justification for this stress modification could be reduced permeability and consequent elevated pore pressure on the plate boundary fault [*Audet et al.*, 2009]. In addition, stresses are tapered to 0.1 of their ambient value near the surface to account for an assumed low stress near the surface. It should be noted that uncertainty in the stress at depth is a very large source of uncertainty in the resulting dynamic earthquake model and tsunami results.

[5] The second part of our modeling method is the tsunami model, which uses a 2D finite difference method to solve the linear long-wave equations [*Shuto*, 1991; *Satake*, 2002]. We take the 3D time-dependent seafloor displacement as a time-dependent boundary condition for our hydrodynamic model, assuming that the water surface is displaced according to the combined effects of vertical and horizontal displacement of the seafloor [*Tanioka and Satake*, 1996]; vertical seafloor displacement is the primary generator of tsunami gravity waves. Use of Kajiura's method [*Kajiura*, 1963] to smooth seafloor displacement made a miniscule difference in our results, and thus was not used in our analysis. Radiation boundary conditions were used along the open-ocean boundary, whereas reflection boundary conditions were used along the 100 m isobath, where nonlinear effects start to become significant [*Shuto*, 1991]. The computational parameters are shown in Table 1.

[6] Propagation from the shallow region of the plate boundary thrust to the splay fault corresponds to the phenomenon of "backwards branching," where rupture approaches a Y-shaped intersection from one of the upper branches rather than the stem. Previous work [e.g., *Kame et al.*, 2003] has indicated that backwards branching is unlikely due to stress shadowing between the two branch segments. However, *Oglesby et al.* [2003a, 2003b] have shown that the presence of a barrier on one branch can cause a stress buildup on the neighboring branch, facilitating backwards branching. To test how rupture may propagate to splay fault segments in subduction zones, we assume in some of our models that there is a barrier (i.e., a zone of increased yield stress) approximately half-way along strike on the plate boundary thrust, from 55 to 120 km along strike. Such a barrier might be provided by a subducted seamount or other structural feature, as inferred by *Cummins and Kaneda* [2000].

## 3. Results

[7] In the following, we compare the results of the homogeneous stress model and the barrier model to investigate how the dynamic faulting process and the resultant tsunami depend on the heterogeneity of the fault stress field. Figure 2 displays the final fault slip on all fault segments for the homogeneous stress model and the barrier model. The homogeneous model produces rupture only on the plate boundary thrust, whereas the barrier model causes rupture to propagate to the splay fault system, as predicted. The parts of the splay fault that overlap slipping regions on the plate boundary thrust are in a stress shadow from the shallow-dipping fault. However, as rupture hits the barrier near the intersection of the splay fault, it increases the shear stress and decreases the clamping normal stress on the splay fault, allowing rupture to propagate on these segments. The homogenous model has a seismic moment of $1.8 \times 10^{21}$ Nm ($M_W$ = 8.2), whereas the barrier model has a significantly smaller seismic moment of $6.8 \times 10^{20}$ Nm ($M_W$ = 7.9). Although the homogeneous model produces a larger earthquake, the steeper dip of the splay fault system produces considerably more vertical surface deformation in the barrier model, as seen in Figure 3. Additionally, the splay faults move the peak surface deformation significantly farther back on the hanging wall, closer to the coast.

[8] The larger vertical motion of the seafloor and its proximity to the shore in the barrier model lead to significant differences between the resultant tsunamis in the two different cases, as shown in Figure 4 (See also Animations S1 and S2 and peak near-shore amplitude in the auxiliary material).[1] The increased vertical seafloor displacement in the barrier model, as well as its more shore-ward location, is directly reflected in the higher amplitude and shorter wavelength in the source region. The barrier model also results in more significant beaming of the tsunami [cf. *Ben-Menahem and Rosenman*, 1972]. The combined effect is to produce much greater wave amplitudes in the nearshore region directly across from the earthquake (i.e., Tosa Bay). Conversely, the homogeneous model produces lower local

[1] Auxiliary materials are available in the HTML. doi:10.1029/2009GL038295.

**Table 1.** Physical and Computational Parameters

| Parameter | Value |
|---|---|
| Density | 3000 kg/m$^3$ |
| $V_P$ | 5477.2 m/s |
| $V_S$ | 3162.3 m/s |
| Static Friction Coefficient | 0.6 |
| Sliding Friction Coefficient | 0.2 |
| Slip-Weakening Parameter | 0.5 m |
| Shear Stress, Fault A | 2.16 MPa |
| Normal Stress, Fault A | 4.78 MPa |
| Shear Stress, Fault B | 3.54 MPa |
| Normal Stress, Fault B | 9.04 MPa |
| Shear Stress, Fault C | 5.69 MPa |
| Normal Stress, Fault C | 12.38 MPa |
| Approximate Finite Element Size | 2000 m |
| Hydrodynamic Grid Size | 1000 m |
| Hydrodynamic Time Step | 0.1 s |

tsunami amplitudes, although slightly higher height farther away on either side, because of the reduced beaming effect.

## 4. Discussion and Conclusions

[9] The results above imply that if rupture initiation is on the plate boundary thrust at a depth shallower than the intersection of a splay fault, rupture propagation to the splay fault (at least one dipping in the same general direction as the main thrust) is difficult due to stress shadowing effects. Effective backwards branching may require some form of barrier or stress heterogeneity along strike, which can reverse the stress shadowing effect on the splay fault. It is tantalizing that in the work of *Cummins and Kaneda* [2000] on the 1946 Nankai earthquake, propagation to the splay fault appeared to take place near a subducted seamount, which may have served as a barrier to further rupture propagation on the plate boundary thrust. In the current models, the corresponding stress field causes significant slip on the splay faults, which in turn leads to a greatly amplified tsunami whose source is closer to shore, compared to that from a homogeneous stress model that ruptures only the plate boundary thrust.

[10] The results above indicate that dynamic fault modeling can add an important new dimension to tsunami modeling. While a dislocation model that includes splay fault slip would similarly produce an amplified tsunami [e.g., *Geist and Yoshioka*, 1996], it would be difficult to predict *a priori* the depth distribution of slip, the probability of splay fault rupture, and the amplitude of slip on the splay fault versus slip on the main thrust. We note that the rupture and slip patterns and the tsunami run-up in our models are not significantly altered by moving the hypocenter down-dip from its current position, emphasizing the point that the generated tsunami is not very sensitive to the temporal details of the rupture. In fact, it is likely that a pure dislocation model with the slip distribution from our dynamic models would produce a very similar tsunami, at least in the medium-to-far field. While it is true that the tsunami itself is not extremely sensitive to the temporal details of the rupture process, the rupture path and final slip pattern in general can be quite sensitive to the temporal evolution of rupture due to the complex stress interactions of the different fault segments [*Harris and Day*, 1993; *Aochi et al.*, 2000; *Anderson et al.*, 2003; *Kame et al.*, 2003; *Oglesby et al.*, 2003b]. Even with the uncertainty in the stress field at depth, dynamic models can help solve these basic seismological questions, which are quite significant for tsunami generation. Dynamic models also can provide a physically consistent framework for relating the earthquake rupture process to tsunami generation. Such models can be used to directly calculate slip distributions from potential future earthquakes, or they can be used to guide the generation of more realistic dislocation models for tsunami prediction. In the future, dynamic faulting models may also be useful for investigating the physics of other tsunami-related faulting effects, such as slow slip in tsunami earthquakes [*Kanamori*, 1972].

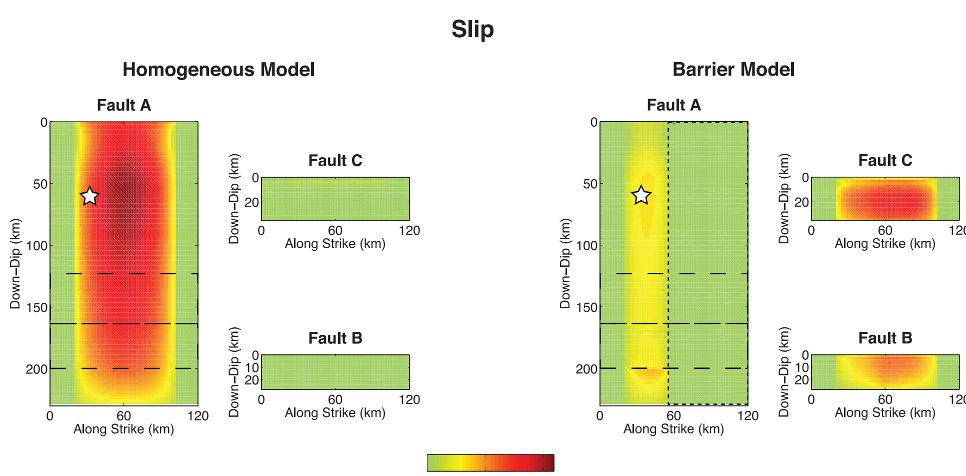


**Figure 2.** Comparison of final slip for (left) homogeneous stress model and (right) barrier model. Rectangles with large dashes show the projection of splay faults B and C onto plate boundary thrust fault A. A rectangle with small dashes (Figure 2, right) indicates the zone of increased friction on fault A in the barrier model. Rupture propagates to the splay fault segments only when a barrier exists on the plate boundary thrust.

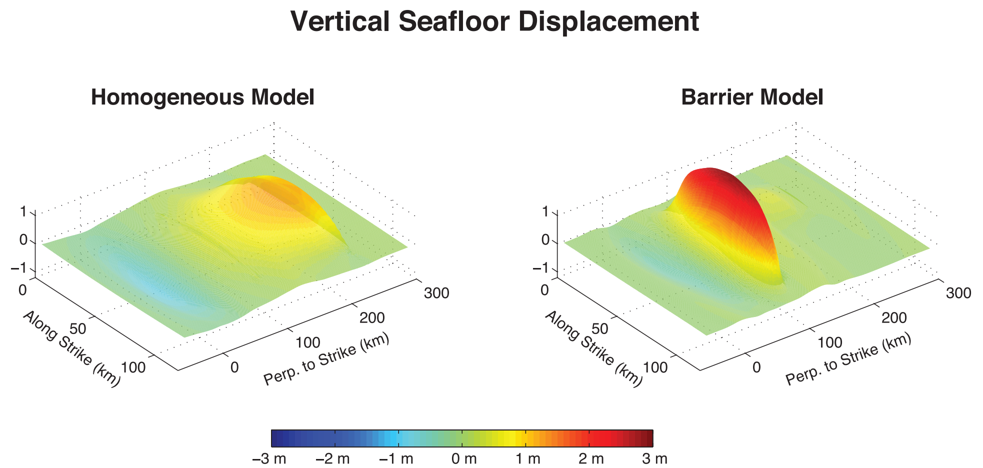


**Figure 3.** Comparison of vertical surface displacement of (left) homogeneous model and (right) barrier model. The steeper dip of the splay fault system produces a greater vertical deformation than the homogeneous model, with peak surface displacement farther back on the hanging wall.

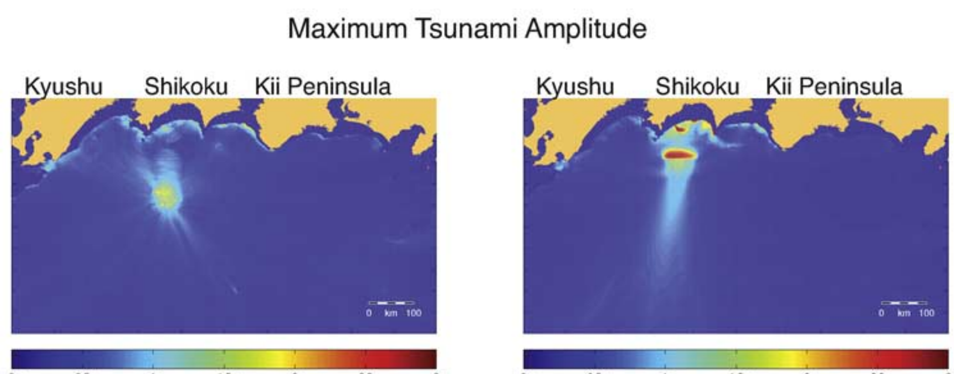


**Figure 4.** Comparison of maximum tsunami wave height in meters for (left) homogeneous model and (right) barrier model. The barrier model's wave height is significantly larger over the fault, and is also larger on the nearby shore. The homogenous model has slightly larger tsunami height on the shore farther away from the fault system because of differences in the radiation pattern for the two tsunamis.

[11] **Acknowledgments.** This work was supported by the Undergraduate Research Program of the Southern California Earthquake Center (SCEC). SCEC is funded by the National Science Foundation (NSF) Cooperative Agreement EAR-0106924. This manuscript was improved by thoughtful conversations with James Rice, Uri ten Brink, and many others.

## References

Anderson, G., B. Aagaard, and K. Hudnut (2003), Fault interactions and large complex earthquakes in the Los Angeles area, *Science*, *302*, 1946–1949, doi:10.1126/science.1090747.

Andrews, D. J. (1976a), Rupture propagation with finite stress in antiplane strain, *J. Geophys. Res.*, *81*, 3575–3582, doi:10.1029/JB081i020p03575.

Andrews, D. J. (1976b), Rupture velocity of plane strain shear cracks, *J. Geophys. Res.*, *81*, 5679–5687, doi:10.1029/JB081i032p05679.

Aochi, H., E. Fukuyama, and M. Matsu'ura (2000), Selectivity of spontaneous rupture propagation on a branched fault, *Geophys. Res. Lett.*, *27*, 3635–3638, doi:10.1029/2000GL011560.

Aochi, H., E. Fukuyama, and R. Madariaga (2002), Effect of normal stress during rupture propagation along nonplanar faults, *J. Geophys. Res.*, *107*(B2), 2038, doi:10.1029/2001JB000500.

Audet, P., M. G. Bostock, N. I. Christensen, and S. M. Peacock (2009), Seismic evidence for overpressured subducted oceanic crust and megathrust fault sealing, *Nature*, *457*, 76–78, doi:10.1038/nature07650.

Baba, T., P. R. Cummins, T. Hori, and Y. Kaneda (2006), High precision slip distribution of the 1944 Tonankai earthquake inferred from tsunami waveforms: Possible slip on a splay fault, *Tectonophysics*, *426*, 119–134, doi:10.1016/j.tecto.2006.02.015.

Ben-Menahem, A., and M. Rosenman (1972), Amplitude patterns of tsunami waves from submarine earthquakes, *J. Geophys. Res.*, *77*, 3097–3128, doi:10.1029/JB077i017p03097.

Bourgeois, J., C. Petroff, H. Yeh, V. V. Titov, C. E. Synolakis, B. Benson, J. Kuroiwa, J. F. Lander, and E. Norabuena (1999), Geologic setting, field survey and modeling of the Chimbote northern Peru, tsunami of 21 February 1996, *Pure Appl. Geophys.*, *154*, 513–540, doi:10.1007/s000240050242.

Cummins, P. R., and Y. Kaneda (2000), Possible splay fault slip during the 1946 Nankai earthquake, *Geophys. Res. Lett.*, *27*, 2725–2728, doi:10.1029/1999GL011139.

Das, S. (1981), Three-dimensional spontaneous rupture propagation and implications for the earthquake source mechanism, *J. Geophys. Res.*, *67*, 375–393.

Day, S. M. (1982), Three-dimensional simulation of spontaneous rupture: The effect of nonuniform prestress, *Bull. Seismol. Soc. Am.*, *72*, 1881–1902.

Fukao, Y. (1979), Tsunami earthquakes and subduction processes near deep-sea trenches, *J. Geophys. Res.*, *84*, 2303–2314, doi:10.1029/JB084iB05p02303.

Geist, E. L., and S. Yoshioka (1996), Source parameters controlling the generation and propagation of potential local tsunamis along the Cascadia margin, *Nat. Hazards*, *13*, 151–177, doi:10.1007/BF00138481.

Harris, R. A., and S. M. Day (1993), Dynamics of fault interaction: Parallel strike-slip faults, *J. Geophys. Res.*, *98*, 4461–4472, doi:10.1029/92JB02272.

Ida, Y. (1972), Cohesive force across the tip of a longitudinal shear crack and Griffith's specific surface energy, *J. Geophys. Res.*, *77*, 3796–3805, doi:10.1029/JB077i020p03796.

Imamura, F., and N. Shuto (1993), Estimate of the tsunami source of the 1992 Nicaraguan earthquake from tsunami data, *Geophys. Res. Lett.*, *20*, 1515–1518, doi:10.1029/93GL01396.

Kajiura, K. (1963), The leading wave of a tsunami, *Bull. Earthquake Res. Inst. Univ. Tokyo*, *41*, 535–571.

Kame, N., J. R. Rice, and R. Dmowska (2003), Effects of pre-stress state and rupture velocity on dynamic fault branching, *J. Geophys. Res.*, *108*(B5), 2265, doi:10.1029/2002JB002189.

Kanamori, H. (1972), Mechanism of tsunami earthquakes, *Phys. Earth Planet. Inter.*, *6*, 346–359, doi:10.1016/0031-9201(72)90058-1.

Moore, G. F., N. L. Bangs, A. Taira, S. Kuramoto, E. Pangborn, and H. J. Tobin (2007), Three-dimensional splay fault geometry and implications for tsunami generation, *Science*, *318*, 1128–1131, doi:10.1126/science.1147195.

Mukoyoshi, H., A. Sakaguchi, K. Otsuki, T. Hirono, and W. Soh (2006), Co-seismic frictional melting along an out-of-sequence thrust in the Simanto accretionary complex. Implications on the tsunamigenic potential of splay faults in modern subduction zones, *Earth Planet. Sci. Lett.*, *245*, 330–343, doi:10.1016/j.epsl.2006.02.039.

Oglesby, D. D. (1999), Earthquake dynamics on dip-slip faults, Ph.D. thesis, Univ. of Calif., Santa Barbara.

Oglesby, D. D. (2005), The dynamics of strike-slip step-overs with linking dip-slip faults, *Bull. Seismol. Soc. Am.*, *95*, 1604–1622, doi:10.1785/0120050058.

Oglesby, D. D., S. M. Day, Y.-G. Li, and J. E. Vidale (2003a), The 1999 Hector Mine earthquake: The dynamics of a branched fault system, *Bull. Seismol. Soc. Am.*, *93*, 2459–2476, doi:10.1785/0120030026.

Oglesby, D. D., S. M. Day, and D. R. H. O'Connell (2003b), The dynamic and static interaction of two thrust faults: A case study with general implications, *J. Geophys. Res.*, *108*(B10), 2489, doi:10.1029/2002JB002228.

Palmer, A. C., and J. R. Rice (1973), The growth of slip surfaces in the progressive failure of overconsolidated clay, *Proc. R. Soc. London, Ser. A*, *332*, 527–548, doi:10.1098/rspa.1973.0040.

Park, J.-O., T. Tsuru, S. Kodaira, P. R. Cummins, and Y. Kaneda (2002), Splay fault branching along the Nankai Subduction Zone, *Science*, *297*, 1157–1160, doi:10.1126/science.1074111.

Satake, K. (1995), Linear and nonlinear computations of the 1992 Nicaragua earthquake tsunami, *Pure Appl. Geophys.*, *144*, 455–470, doi:10.1007/BF00874378.

Satake, K. (2002), Tsunamis, in *International Handbook of Earthquake and Engineering Seismology, Part A*, edited by W. H. K. Lee et al., pp. 437–451, Academic, San Diego, Calif.

Shuto, N. (1991), Numerical simulation of tsunamis: Its present and near future, *Nat. Hazards*, *4*, 171–191, doi:10.1007/BF00162786.

Tanioka, Y., and K. Satake (1996), Tsunami generation by horizontal displacement of ocean bottom, *Geophys. Res. Lett.*, *23*, 861–865, doi:10.1029/96GL00736.

Whirley, R. G., and B. E. Engelmann (1993), *DYNA3D: A Nonlinear, Explicit, Three-Dimensional Finite Element Code for Solid and Structural Mechanics—User Manual*, Lawrence Livermore Natl. Lab., Livermore, Calif.

E. L. Geist, U.S. Geological Survey, Mail Stop 999, 345 Middlefield Road, Menlo Park, CA 94025, USA.

D. D. Oglesby, Department of Earth Sciences, University of California, 900 University Avenue, Riverside, CA 92521-0423, USA. (david.oglesby@ucr.edu)

J. Wendt, Department of Physics, Pomona College, 333 North College Way, Claremont, CA 91711, USA.